A protein kinase binds the C-terminal domain of the readthrough protein of Turnip yellows virus and regulates virus accumulation

Caren Rodriguez-Medina, Sylvaine Boissinot, Sophie Chapuis, Dalya Gereige, Maryam Rastegar, Monique Erdinger, Frederic Revers, Véronique Ziegler-Graff, Véronique Brault

▶ **To cite this version:**

Caren Rodriguez-Medina, Sylvaine Boissinot, Sophie Chapuis, Dalya Gereige, Maryam Rastegar, et al.. A protein kinase binds the C-terminal domain of the readthrough protein of Turnip yellows virus and regulates virus accumulation. Virology, 2015, 486, pp.44-53. 10.1016/j.virol.2015.08.031 . hal-02640267

HAL Id: hal-02640267
https://hal.inrae.fr/hal-02640267v1

Submitted on 28 May 2020

HAL is a multi-disciplinary open access archive for the deposit and dissemination of scientific research documents, whether they are published or not. The documents may come from teaching and research institutions in France or abroad, or from public or private research centers.

L'archive ouverte pluridisciplinaire **HAL**, est destinée au dépôt et à la diffusion de documents scientifiques de niveau recherche, publiés ou non, émanant des établissements d'enseignement et de recherche français ou étrangers, des laboratoires publics ou privés.

Virology 486 (2015) 44–53

Contents lists available at ScienceDirect

Virology

journal homepage: www.elsevier.com/locate/yviro

A protein kinase binds the C-terminal domain of the readthrough protein of *Turnip yellows virus* and regulates virus accumulation

Caren Rodriguez-Medina [a,1,4], Sylvaine Boissinot [a,4], Sophie Chapuis [b], Dalya Gereige [a,2], Maryam Rastegar [a,3], Monique Erdinger [a], Frédéric Revers [c], Véronique Ziegler-Graff [b], Véronique Brault [a,*]

[a] UMR 1131 SVQV INRA-UDS, 28 rue de Herrlisheim, 68021 Colmar, France
[b] Institut de Biologie Moléculaire des Plantes, Laboratoire propre du CNRS conventionné avec l'Université de Strasbourg, 12 rue du Général Zimmer, 67084 Strasbourg, France
[c] INRA, Université de Bordeaux, UMR 1332 de Biologie du Fruit et Pathologie, 33882 Villenave d'Ornon, France

ARTICLE INFO

Article history:
Received 28 May 2015
Returned to author for revisions
20 June 2015
Accepted 29 August 2015

Keywords:
Plant
Polerovirus
Phloem
Movement
Kinase
CIPK

ABSTRACT

Turnip yellows virus (TuYV), a phloem-limited virus, encodes a 74 kDa protein known as the readthrough protein (RT) involved in virus movement. We show here that a TuYV mutant deleted of the C-terminal part of the RT protein (TuYV-ΔRT_{Cter}) was affected in long-distance trafficking in a host-specific manner. By using the C-terminal domain of the RT protein as a bait in a yeast two-hybrid screen of a phloem cDNA library from *Arabidopsis thaliana* we identified the calcineurin B-like protein-interacting protein kinase-7 (AtCIPK7). Transient expression of a GFP:CIPK7 fusion protein in virus-inoculated *Nicotiana benthamiana* leaves led to local increase of wild-type TuYV accumulation, but not that of TuYV-ΔRT_{Cter}. Surprisingly, elevated virus titer in inoculated leaves did not result in higher TuYV accumulation in systemic leaves, which indicates that virus long-distance movement was not affected. Since GFP:CIPK7 was localized in or near plasmodesmata, CIPK7 could negatively regulate TuYV export from infected cells.

© 2015 Elsevier Inc. All rights reserved.

Introduction

Turnip yellows virus (TuYV), previously referred to as *Beet western yellows virus* (BWYV), is a polerovirus belonging to the *Luteoviridae* family. These phloem-limited plant viruses are transmitted by aphids and possess a small (5.6–6 kb) plus sense-RNA genome protected by an icosahedral capsid of about 25 nm. The viral particles are composed of two structural proteins: the major coat protein of 22 kDa (CP) and a minor component of ca. 54 kDa referred to as the readthrough (RT*) protein (Gildow, 1999). The RT* protein arises from a C-terminal cleavage of the full-length precursor RT protein of 74 kDa synthesized after ribosomes bypass the CP stop codon. Both CP and RT* structural proteins are involved in virus movement and aphid transmission (Brault et al., 1995; Bruyère et al., 1997; Chay et al., 1996; Mutterer et al., 1999; Peter et al., 2009, 2008; Wang et al., 1995). Involvement of the full-length RT protein of TuYV in virus movement was previously demonstrated by monitoring *in planta* progression of viral mutants either unable to synthesize the RT protein or bearing small deletions in the C-terminal domain (Brault et al., 1995; Bruyère et al., 1997). More recently the RT protein was shown to play a role in *Potato leafroll virus* (PLRV) phloem limitation (Peter et al., 2009). An additional viral protein (P4) encoded by ORF4 is involved in polerovirus movement. P4 possesses characteristics of conventional movement proteins (Schmitz et al., 1997; Sokolova et al., 1997; Tacke et al., 1991, 1993) and its involvement in polerovirus movement was reported to be host-specific (Lee et al., 2002; Ziegler-Graff et al., 1996).

To accomplish their infection cycle in the plant, poleroviruses rely on specific interactions with host cellular proteins but so far only a few partners of polerovirus proteins have been identified. The P0 protein encoded by TuYV and *Cucurbit aphid-borne yellows virus* (CABYV) was shown to bind, *in vitro* and in yeast, to components of the SCF family of ubiquitin E3 ligases, namely ASK1 and ASK2 proteins (Pazhouhandeh et al., 2006). These interactions induce the degradation of AGO1, the major component of the RNA-induced silencing complex, leading to suppression of the plant's

* Corresponding author.
E-mail address: veronique.brault@colmar.inra.fr (V. Brault).
[1] Present address: Corporación Colombiana de Investigación Agropecuaria, Tibaitatá, Colombia.
[2] Present address: Lebanese University, Faculty of Science 3, Tripoli, Lebanon.
[3] Present address: Shiraz University, Plant Protection Department, Shiraz, Iran.
[4] Both authors contributed equally.

http://dx.doi.org/10.1016/j.virol.2015.08.031
0042-6822/© 2015 Elsevier Inc. All rights reserved.

viral-targeted cellular defenses (Baumberger et al., 2007; Bortolamiol et al., 2007; Csorba et al., 2010). Translation initiation factors from the eIF4G and eIF4E families have recently been shown to play a role in the infection cycle of, respectively, TuYV and *Beet mild yellowing virus* (BMYV) in *A. thaliana* and to directly interact in yeast with the viral genome-linked protein (Reinbold et al., 2013). Finally the PLRV P4 protein was reported to be phosphorylated *in vitro* by a membrane-associated protein kinase (Sokolova et al., 1997), but its specific role in the virus cycle *in planta* has not been demonstrated.

To obtain more insights into the function of the RT protein in polerovirus movement and in particular to decipher the role of the C-terminal domain of the protein, we analyzed virus accumulation *in planta* of a TuYV mutant deleted of the C-terminal part of the RT. We found that this domain is involved in TuYV long-distance movement in a host-specific manner. By screening a phloem cDNA library from *A. thaliana* using the C-terminal domain of the RT protein as a bait, we identified calcineurin B-like-interacting protein kinase 7 (AtCIPK7) as a putative interacting partner. Transient over-expression of AtCIPK7 in leaves promoted a local increase in virus accumulation, which had no beneficial effect on virus long-distance movement. The fusion protein GFP:CIPK7 was detected in or in close proximity of plasmodesmata suggesting a key role of AtCIPK7 in regulating virus export from the infected cell.

Results

Role of the C-terminal domain of the RT protein of TuYV in the viral cycle

To investigate more precisely the function of the C-terminal domain of the TuYV-RT protein (RT_{Cter}) in the virus cycle, a deletion was introduced downstream of a position (lysine 437) identified by mass spectrometry as the last C-terminal amino acid of the RT* (Revollon et al., 2010). The deletion starts at glutamine at position 471, since we previously showed that a nucleotide sequence encompassing lysine 437 was strictly required for the readthrough mechanism of the CP (Bruyère et al., 1997), and ends at the last amino acid of the RT protein (phenylalanine 670). The deletion was generated in the RT sequence of TuYV-NM, a wild-type virus variant in which two unique restriction sites were introduced into the RT sequence (Fig. 1A) (Brault et al., 2005). The deletion mutant, designed hereafter as TuYV-ΔRT_{Cter}, was lacking the 200 C-terminal amino acids of the RT protein (Fig. 1A). *In vitro* synthesized transcripts of TuYV-ΔRT_{Cter} were fully competent for replication in plant protoplasts and produced a truncated RT protein of about 60 kDa migrating slightly above the RT* (Fig. 1B).

To address the ability of TuYV-ΔRT_{Cter} to infect whole plants, the virus mutant was introduced into a binary vector under the control of the *Cauliflower mosaic virus* (CaMV) 35S promoter and inoculated to different plant species. When assayed by DAS-ELISA, TuYV-ΔRT_{Cter} accumulated in agroinfiltrated leaves of *Montia perfoliata* and *N. benthamiana* at a level close to TuYV-NM and TuYV-WT (Table S1). This comparable accumulation in *M. perfoliata* was confirmed by Western-blot showing similar levels of CP accumulation in leaves infiltrated with TuYV-WT or TuYV-ΔRT_{Cter} (data not shown). Virus titer was then measured on young non-inoculated leaves of *M. perfoliata*, *A. thaliana* and *N. benthamiana* 4 weeks after inoculation. TuYV-ΔRT_{Cter} was infectious in *M. perfoliata* and *A. thaliana* however at a lower level compared to TuYV-WT and -NM but the mutant was unable to systemically infect *N. benthamiana* (Table 1). TuYV-ΔRT_{Cter} accumulation in systemic leaves of *M. perfoliata* remained at a low level during eight weeks in three independent experiments (Table S2). In contrast to what was previously reported for a PLRV mutant lacking the C-terminal part of the RT protein (Peter et al., 2009), TuYV-ΔRT_{Cter} was unable to escape from phloem cells (data not shown). Our results show that long-distance movement of TuYV-ΔRT_{Cter} is reduced, or even completely inhibited as observed in *N. benthamiana*, suggesting an important function of RT_{Cter} in long-distance movement of TuYV. Moreover this function seems host-specific.

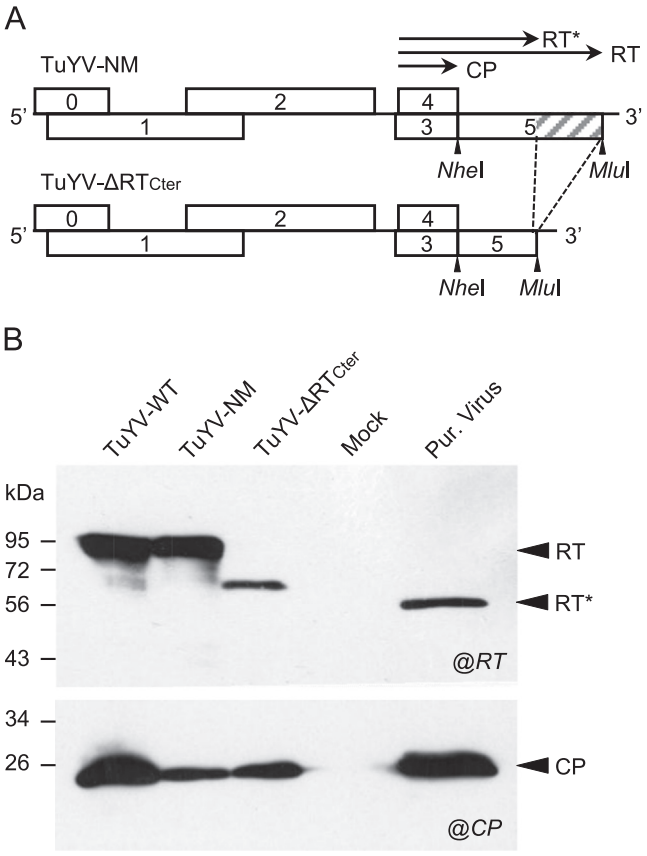

Fig. 1. (A) Schematic representation of TuYV-ΔRT_{Cter} with the position of the encoded structural proteins (CP and RT*) and the full-length RT protein (RT). The gray hatched area at RT_{Cter} of TuYV-NM has been deleted in TuYV-ΔRT_{Cter}. Positions of the introduced restriction sites NheI and MluI in TuYV-NM and in TuYV-ΔRT_{Cter} are indicated. (B) Western blot analysis of TuYV capsid proteins in transcript-infected *C. quinoa* protoplasts. The upper portion of the blot was incubated with an antiserum raised against the ORF5-encoding protein and the CP protein was detected in the lower portion of the blot using antibodies raised against TuYV-CP. Position of the molecular weight markers is indicated on the left. Mock: Mock-inoculated protoplasts; Pur. Virus: Purified TuYV-WT; @: antibody.

CIPK7 from A. thaliana is a potential phloem-partner of the C-terminal domain of the TuYV RT protein

In order to unravel the function of RT_{Cter} in the phloem-restricted infection cycle of TuYV, we looked for cellular partners of this viral domain. A phloem enriched cDNA library of *A. thaliana* was directly constructed in *Saccharomyces cerevisiae* strain Y187, using total RNA extracted from companion cell protoplasts. These phloem enriched cells were isolated from transgenic *A. thaliana* expressing the GFP under the control of the AtSUC2 companion cell promoter (Imlau et al., 1999). Fluorescent protoplasts were sorted by Fluorescence Activated Cell Sorting (FACS) and sorting efficacy was controlled by measuring expression of companion cell specific genes by real-time PCR (Chapuis et al., in preparation). The cDNA library cloned into the pGADT7 vector contained an average insert size of about 750 nucleotides and had a titer of 1.5×10^7 cfu/ml. The TuYV-RT_{Cter} was expressed as a fusion with the GAL4 DNA binding domain (BD) in Y2HGold yeast strain and subsequently used as a

Table 1
Virus accumulation of TuYV-ΔRT$_{Cter}$ in non-inoculated leaves of *M. perfoliata*, *A. thaliana* and *N. benthamiana* following agroinfiltration.

	M. perfoliata		*A. thaliana*				*N. benthamiana*	
			Exp. 1		*Exp. 2*			
	nb inf./total inoc.[a]	OD ± SD[b]	nb inf./total inoc.[a]	OD ± SD[b]	nb inf./total inoc.[a]	OD ± SD[b]	nb inf./total inoc.[a]	OD ± SD[b]
TuYV-ΔRT$_{Cter}$	10/15	[#]0.51 ± 0.26	7/30	0.21 ± 0.07	6/15	0.46 ± 0.25	0/12	0.11 ± 0.00
TuYV-NM	14/15	1.61 ± 0.12	[d]/	/	/	/	/	/
TuYV-WT	14/15	1.85 ± 0.23	27/30	1.86 ± 0.33	13/15	1.71 ± 0.20	12/12	1.64 ± 0.25
Non-inoc.[c]	0/1	0.13	0/6	0.14 ± 0.01	0/4	0.13 ± 0.01	0/3	0.12 ± 0.00

[a] Number of infected plants/number of plants agroinfiltrated. A plant is considered infected when the ELISA value of the leaf extract is above the ELISA value of three non-infected plants +3 times the standard deviation of these extracts. DAS–ELISA was done 4 wpi.
[b] Mean absorbance value at 405 nm of the infected plants ± Standard Deviation.
[c] Non-inoculated plants. The OD value corresponds to the mean absorbance of all plants.
[d] Not done.
[#] The calculated *P*-value after Kruskal–Wallis analysis (R commander) to compare TuYV-ΔRT$_{Cter}$ accumulation with TuYV-WT or -NM is below 0.05 meaning that accumulation of TuYV-ΔRT$_{Cter}$ is statistically different from those of TuYV-WT and –NM.

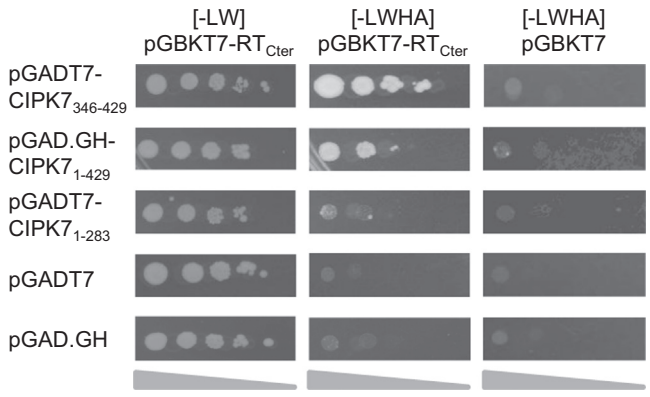

Fig. 2. Interaction between RT$_{Cter}$ of TuYV and AtCIPK7 in yeast cells. The yeast strain Y2HGold was co-transformed with pGBKT7-RT$_{Cter}$ and one of the following constructs: pGADT7-CIPK7$_{346-429}$, pGAD.GH-CIPK7-FL$_{1-429}$, pGADT7-CIPK7$_{1-283}$ or the empty pGADT7 and pGAD.GH vectors. Alternatively the pGAD-derived constructs were combined in yeast with the empty pGBKT7 vector. Ten-fold serial dilutions (from 1 to 10^{-4}) of doubly transformed cells were allowed to grow on a medium lacking leucine and tryptophan [-LW] before being transferred onto a selective medium deprived of leucine, tryptophane, histidine and adenine [-LWHA]. Yeast cells were allowed to grow for 8 days at 23 °C.

bait. Screening of the phloem cDNA library was performed by yeast mating. A cDNA clone encoding the C-terminal sequence of the CIPK7 from *A. thaliana* referred thereafter as AtCIPK7 (AT3G23000, residues 346-429) was identified as a potential interacting partner of the viral domain. CBL-interacting protein kinases (CIPKs) are a group of serine/threonine protein kinases that interact with the Ca^{2+} sensors Calcineurin B-like proteins (CBLs) (Kolukisaoglu et al., 2004; Weinl and Kudla, 2009). *AtCIPK7* is expressed in all cell types including phloem cells (Hruz et al., 2008). Vascular expression of this gene was confirmed by analyzing RNAseq data from *A. thaliana* companion cells-enriched RNA (Chapuis, personal communication). To confirm the interaction, the plasmid bearing the partial AtCIPK7 cDNA sequence (referred to hereafter as pGAD-CIPK7$_{346-429}$) was introduced into Y2HGold yeast strain together with pGBKT7-RT$_{Cter}$. Serial dilutions of the co-transformed cells were plated onto a medium lacking leucine and tryptophan [-LW], to allow yeast growth after transformation, and onto the [-LWHA] medium (LW medium deprived of histidine and adenine) to select yeast cells in which *in vivo* interactions occurred (Fig. 2). Interestingly, we observed that RT$_{Cter}$ was able to interact with the full-length AtCIPK7, a protein of 429 amino acids, but not with the first 283 N-terminal amino acids of AtCIPK7 (Fig. 2). No yeast growth was observed on [-LWHA] medium when pGBKT7-RT$_{Cter}$ was co-transformed with empty pGADT7 or pGAD.GH vectors. These results show that RT$_{Cter}$ preferentially binds a region localized at the C-terminus of AtCIPK7. This interaction was specific because no binding was recorded in yeast between the C-terminal domain of AtCIPK7 and the major (CP) and minor (RT*) coat proteins of TuYV. Interaction between AtCIPK7 and the complete RT protein could not be assessed because the full-length readthrough domain of the protein activated transcription of both *ADE2* and *HIS3* reporter genes when expressed alone (data not shown).

Detecting interaction of AtCIPK7 and RT$_{Cter}$ transiently expressed via agroinfiltration

To confirm the physical interaction between the C-terminal domain of AtCIPK7 and the RT$_{Cter}$, GFP was fused to the N-terminus of AtCIPK7 (GFP:CIPK7) and expressed transiently with RFP:RT$_{Cter}$ by agroinfiltration in *N. benthamiana*. The cell extracts were immunopurified with anti-GFP beads to pull down GFP:CIPK7-complexes, and the immunoprecipitated products were fractionated by SDS-PAGE and detected with anti-RFP or anti-GFP antibodies. RFP:RT$_{Cter}$ of 53 kDa expected molecular weight was detected in the leaf extracts together with a larger product of ca 60 kDa (Fig. 3A left panel) which may correspond to a post-translational modified form of the protein. The two products corresponding to RFP:RT$_{Cter}$ were detected in the immunocaptured complex together with GFP:CIPK7 (Fig. 3A, right panel). No such products were present in the leaf extracts infiltrated with GFP and RFP:RT$_{Cter}$ (Fig. 3A, right panel). To verify that the complex formation was due to an interaction of GFP:CIPK7 with RT$_{Cter}$ and not with RFP, we performed the same assay replacing the RFP:RT$_{Cter}$ construct by RFP in the agroinfiltration experiment. No RFP protein was immunoprecipitated when GFP:CIPK7 was present (Fig. 3A, right panel) confirming the specific interaction between CIPK7 and RT$_{Cter}$. The presence of the GFP:CIPK7 on the anti-GFP beads was moreover confirmed by the detection of the fusion protein of 73 kDa in the leaf extracts infiltrated with GFP:CIPK7 construct (Fig. 3B, right panel). This experiment confirmed that GFP:CIPK7 interacts with RT$_{Cter}$.

Effect of expression inhibition of AtCIPK7 on TuYV accumulation

To address the function of AtCIPK7 in the TuYV cycle, we first analyzed virus accumulation in an *A. thaliana cipk7* knock-out mutant (T-DNA insertion, SALK_124117). The T-DNA insertion encompasses the 3' terminal coding and non-coding sequences of *AtCIPK7*. The absence of *AtCIPK7* mRNA detection in the *cipk7* mutant was confirmed by RT-PCR (Fig. S1). Homozygous plants were inoculated with TuYV using viruliferous aphids, and viral

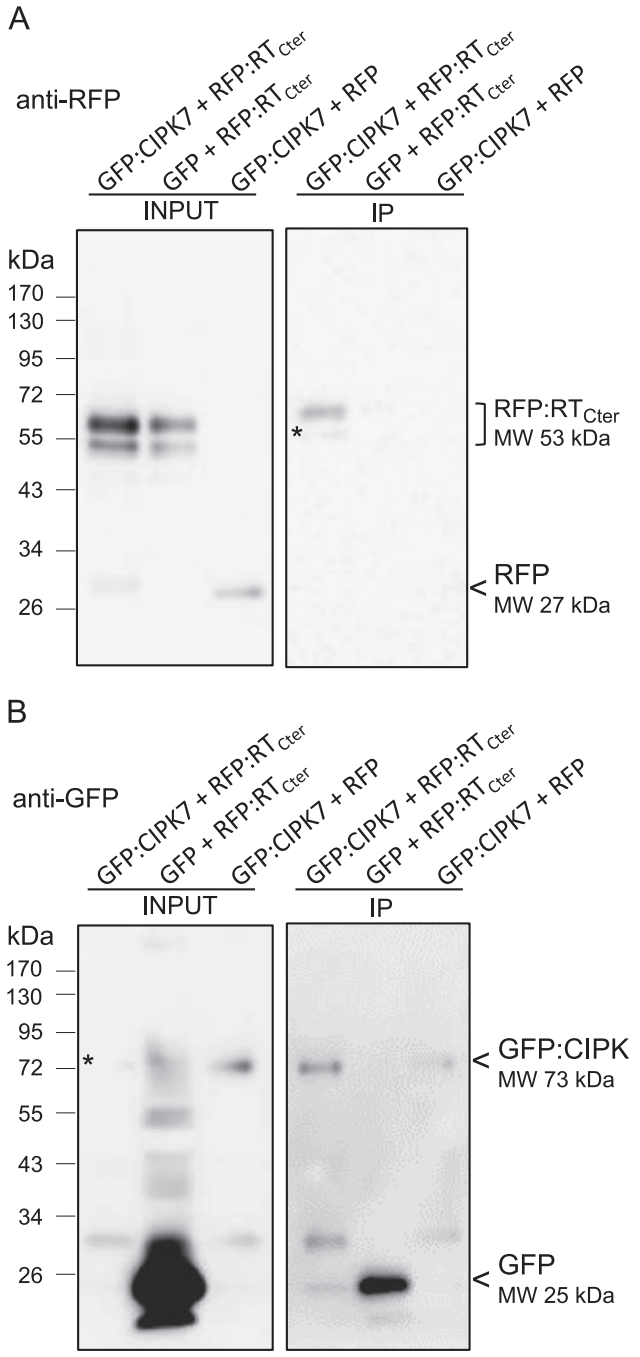

Fig. 3. Interaction between RT_{Cter} of TuYV and AtCIPK7 in *N. benthamiana*. Different cell lysates were immunoprecipitated with anti-GFP beads separated by SDS-PAGE and immunoblotted with anti-RFP (A) or anti-GFP (B). I: input; E: eluate; FT: flow through; *: faint band in (A) first panel. Position of the molecular weight markers is indicated on the left. MW: expected protein molecular weight.

accumulation was measured three weeks post-inoculation in the non-inoculated leaves by DAS-ELISA. In two independent experiments, no significant difference in virus accumulation was observed in *cipk7* when compared with TuYV accumulation in Col-0 (Table S3). Genome analysis identified at least 25 *CIPK* genes in *A. thaliana* (Kolukisaoglu et al., 2004; Weinl and Kudla, 2009), and CIPK4 displays the highest homology with CIPK7 (73% of amino acid identity). Functional redundancy between the different CIPK proteins is likely, which may explain the absence of differential virus accumulation between *cipk7* and Col-0 plants.

Effect of over-expression of AtCIPK7 on TuYV accumulation

In another set of experiments, we investigated the effect of overexpression of AtCIPK7 on TuYV accumulation. *N. benthamiana* leaves were co-infiltrated with a TuYV full-length clone together with the AtCIPK7 fusion construct where GFP was placed at the N-terminus of the protein (GFP:CIPK7). As controls, leaves were co-infiltrated with the viral clone and the free GFP or the AtCIPK7 fused to GFP at its C-terminus (CIPK7:GFP). Expression of the AtCIPK7-GFP fusion proteins was confirmed by Western-blot three days after infiltration (Fig. S2). Virus accumulation could not be assessed in infiltrated leaves by real-time RT-PCR because of the presence of viral transcripts deriving from the *Cauliflower mosaic virus* (CaMV)-35S promoter provided by the recombinant agrobacteria. We therefore used DAS-ELISA to evaluate virus titer since the structural proteins (measured in this assay) are expressed from the sub-genomic RNA and thus substantiate genuine viral replication. When TuYV was co-expressed with CIPK7:GFP or with free GFP, no statistical difference (Kruskal–Wallis analysis, *P*-value$>$0.05) in virus accumulation was observed three days post-inoculation in infiltrated tissue (Fig. 4A). Conversely, when GFP was positioned at the N-terminus of AtCIPK7 (GFP:CIPK7) releasing a free AtCIPK7 C-terminus, co-expression of this protein with the virus caused a significant increase in TuYV accumulation in infiltrated tissue (Kruskal–Wallis analysis, *P*-value$<$0.05). This fostering local effect of GFP:CIPK7 expression on the TuYV titer was observed in three additional independent experiments (Fig. S3) with a significant virus increase when the fusion protein was present. In order to evaluate the ratio of such increase, an additional independent experiment was performed where the tested leaf samples were diluted and the OD values were referred to a linear standard curve of known amounts of TuYV virions loaded on the same microplate. The raise in virus accumulation reached a 16 fold increase in the presence of GFP:CIPK7 (Fig. 4B). A similar stimulating effect of AtCIPK7 on virus accumulation was observed with BMYV, a closely related polerovirus (Fig. S4). In contrast to TuYV, both CIPK7-GFP constructs induced a moderate increase of BMYV accumulation (2 times more virus when AtCIPK was over-expressed) (Fig. S4).

In order to assess whether the effect of AtCIPK7 on local virus accumulation was linked to its ability to bind RT_{Cter}, TuYV-ΔRT_{Cter} was co-infiltrated in *N. benthamiana* leaves with GFP:CIPK7 or GFP as a control. As shown in Fig. 4C, no stimulating effect of GFP:CIPK was observed on TuYV-ΔRT_{Cter} titer in infiltrated leaves while an increase of TuYV-WT accumulation was visible when the AtCIPK7-fusion protein was present. The results of a second experiment are shown in Fig. S5. Together these data clearly indicate that RT_{Cter} domain is essential to foster AtCIPK7's action on virus accumulation in inoculated leaves. When leaves are agroinoculated, epidermal and mesophyll cells are mostly targeted but we assume that the stimulatory effect of AtCIPK7 on TuYV accumulation, observed in these cells, occurs also in phloem cells.

To investigate whether the TuYV titer increase monitored in leaves transiently expressing GFP:CIPK7 would affect viral long-distance movement, and further accumulation in systemic leaves, upper non-infiltrated leaves of plants co-infiltrated with TuYV and GFP:CIPK7 or TuYV and GFP constructs, were assayed by DAS-ELISA three to four weeks post-inoculation in two independent experiments. Surprisingly, the higher accumulation of TuYV observed in leaves co-infiltrated with GFP:CIPK did not result in elevated virus titer in systemic leaves (Table 2). A lower level of virus accumulation was even observed in one experiment when GFP:CIPK was co-expressed with TuYV (Table 2, Exp. 1). These results show that a higher local TuYV titer in infiltrated leaves transiently overexpressing GFP:CIPK7 did not lead to an increase in virus accumulation in systemic leaves.

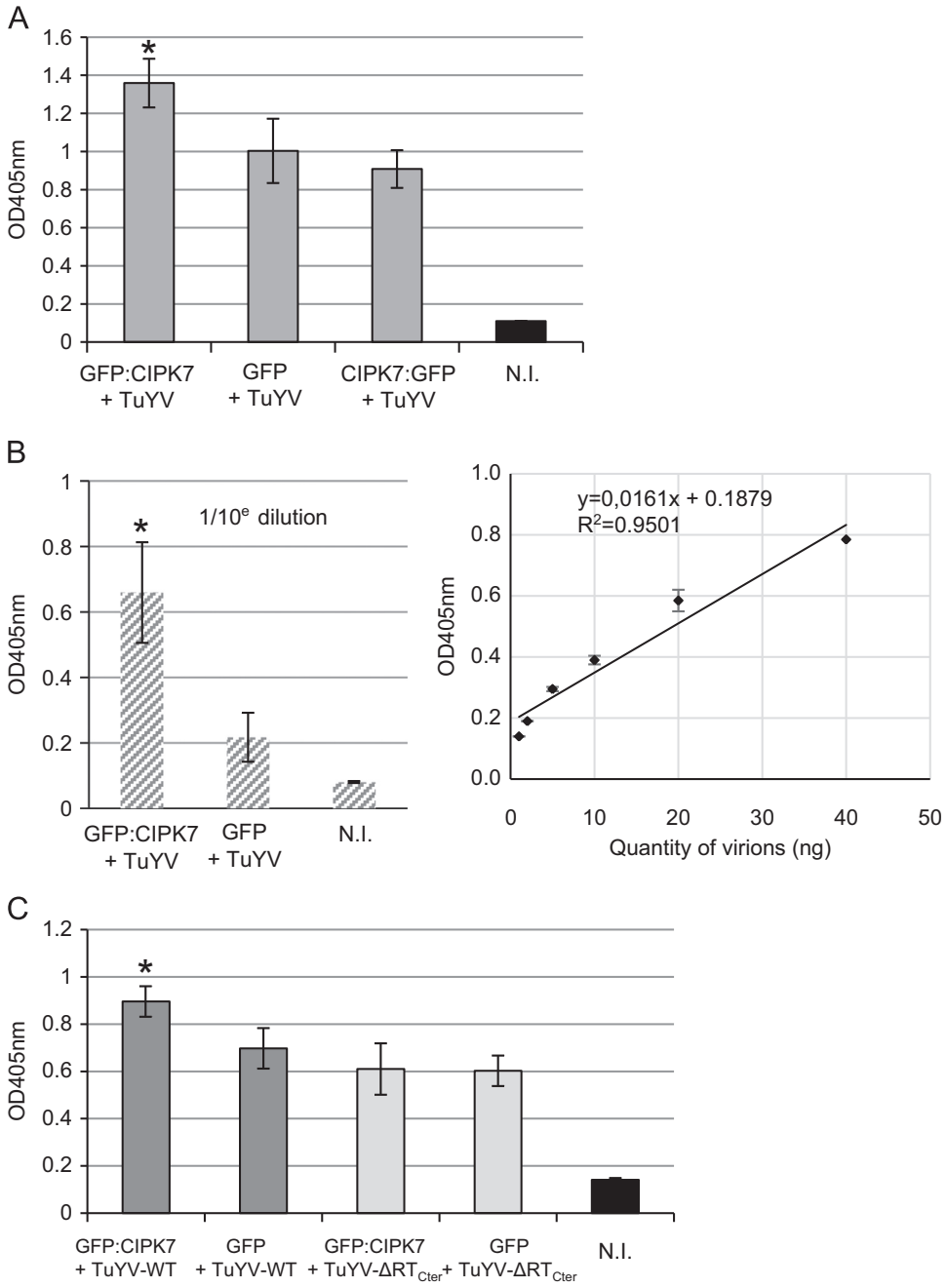

Fig. 4. (A) Accumulation of TuYV in *N. benthamiana* leaves infiltrated with TuYV and AtCIPK7 fused to GFP. AtCIPK7 was tagged to GFP at its N- or C-terminus (GFP:CIPK7 and CIPK7:GFP, respectively). (B) Evaluation of TuYV accumulation in agroinfiltrated leaves. The experiment was done as in A except that a dilution of 1/10 of the leaf samples were deposited on the plate. On the right side, standard curve calibration made from serial dilutions of purified virus (TuYV). The absorbance values were measured 12 min after substrate incubation. (C) Accumulation of TuYV-ΔRT_{Cter} in *N. benthamiana* leaves infiltrated with GFP:CIPK7. As a control, TuYV wild-type virus was inoculated together with GFP:CIPK7. Virus titer in agroinfiltrated leaves was analyzed by DAS-ELISA at 3 dpi. Each histogram represents the mean absorbance value at 405 nm of 10 (A) or 12 (C) plants. *: The calculated *P*-value after Kruskal–Wallis analysis (R commander) to compare TuYV accumulation in leaves infiltrated with GFP:CIPK7 with virus accumulation in leaves infiltrated with the free GFP is below 0.05, meaning that TuYV-WT accumulation is statistically different under these two conditions. N.I.: non-infiltrated leaves.

The CIPK7 localizes to plasmodesmata

In order to examine the subcellular localization of both fusion proteins, GFP:CIPK7 and CIPK7:GFP, *N. benthamiana* leaves were agroinfiltrated with the corresponding constructs and epidermal cells were observed by confocal microscopy 48 h post-infiltration. GFP:CIPK7 was localized in the nucleus and the cytoplasm (Fig. 5A). Interestingly, GFP:CIPK7 co-localized with the plasmodesmata marker PDLP1 fused to RFP (Amari et al., 2010) suggesting that GFP-CIPK might be located in or near plasmodesmata (Fig. 5A, second row, three right panels). On the other hand, the CIPK7:GFP construct, which had no visible effect on virus accumulation, was present in the nucleus and the cytoplasm and was never observed in plasmodesmata (Fig. 5B). These observations point to a correlation between the plasmodesmata targeting of GFP:CIPK7 and its biological effect on virus accumulation.

Regulation of AtCIPK7 mRNA upon infection with TuYV

Since we observed that overexpression of GFP-CIPK7 affected TuYV accumulation, we addressed the issue of a putative feedback effect of TuYV infection on the expression of AtCIPK7 mRNA.

To answer this question accumulation of AtCIPK7 transcripts was quantified by qRT-PCR in *A. thaliana* plants inoculated with TuYV using viruliferous aphids. *Myzus persicae* were allowed to acquire purified virus particles from an artificial diet before being transferred onto *A. thaliana* Col-0 plants. As a control, aphids fed on the artificial diet free of virions were similarly deposited onto test plants. Aphids were eliminated by an insecticide treatment four days after loading and RNA was extracted from newly developed leaves 10 or 21 days post-aphid infestation (dpai). The presence of viral RNA in systemic leaves of individual plants was first tested by RT-PCR before combining the RNA samples of infected plants for qRT-PCR analysis. While no difference in *AtCIPK7* expression was observed among infected and non-infected plants 10 dpai, a moderate reduction (20%) of AtCIPK7 mRNA accumulation was detected 21 dpai (Fig. S6).

Table 2
Virus accumulation of TuYV-WT in non-inoculated leaves of *N. benthamiana* following agroinfiltration with GFP:CIPK7.

	Exp. 1		Exp. 2	
	nb inf./inoc.[a]	OD ± SD[b]	nb inf./inoc.[a]	OD ± SD[b]
TuYV-WT + GFP:CIPK	12/12	[#]1.40 ± 0.12	10/15	0.64 ± 0.15
TuYV-WT + GFP	12/12	1.64 ± 0.25	12/15	0.60 ± 0.21
Non-inoc.[c]	0/3	0.12 ± 0.00	0/3	0.11 ± 0.01

[a] Number of infected plants/number of plants agroinfiltrated. A plant is considered infected when the ELISA value of the leaf extract is above the ELISA value of three non-infected plants +3 times the standard deviation of these extracts. DAS-ELISA was done at 3 (Exp.1) and 4 (Exp.2) wpi.

[b] Mean absorbance value at 405 nm of the infected plants ± Standard Deviation.

[c] Non-inoculated plants. The OD value corresponds to the mean absorbance of all plants.

[#] The calculated *P*-value after Kruskal–Wallis analysis (R commander) to compare accumulation of TuYV-WT is below 0.05 meaning that virus accumulation is statistically lower in this experiment when the virus is inoculated with GFP:CIPK compared to GFP alone.

Discussion

By analyzing infectivity of a TuYV mutant deleted in the RT gene, we disclosed that the RT_{Cter} domain is involved in long-distance transport of the virus. This domain is not strictly required for propagation to non-inoculated tissue of *M. perfoliata* and *A. thaliana*, but it appeared to be mandatory for systemic infection of *N. benthamiana*, suggesting a host-specific effect of RT_{Cter}. Recently, we showed that RT_{Cter} of CABYV, another polerovirus, is strictly required for systemic movement in all the hosts tested including *M. perfoliata* and *A. thaliana* (Boissinot et al., 2014). This indicates that long-distance movement of poleroviruses relies on different viral determinants which may vary depending on the host.

Screening a phloem enriched cDNA library by yeast two-hybrid led to the identification of AtCIPK7 as a potential cellular partner of the RT_{Cter} domain of TuYV. The binding domain of the kinase protein is located at the C-terminal part. Interaction between AtCIPK7 and the RT_{Cter} was further confirmed *in planta*. AtCIPK7 belongs to a group of serine/threonine protein kinases which interact with the Ca^{2+} sensors, the Calcineurin B-like proteins (CBL) (Kudla et al., 1999). CBLs and CIPKs form complexes that are involved in plant response to environmental signals, particularly salt and osmotic stress (Batistic and Kudla, 2012; D'Angelo et al., 2006; Halfter et al., 2000; Liu et al., 2000; Quan et al., 2007; Shi et al., 2000; Weinl and Kudla, 2009). Genome-wide analyzes identified at least 10 CBL and 25 CIPK genes in *A. thaliana* (Kolukisaoglu et al., 2004; Weinl and Kudla, 2009). CIPKs have a two-domain structure, consisting of a highly conserved N-terminal kinase domain and a variable C-terminal regulatory domain. This

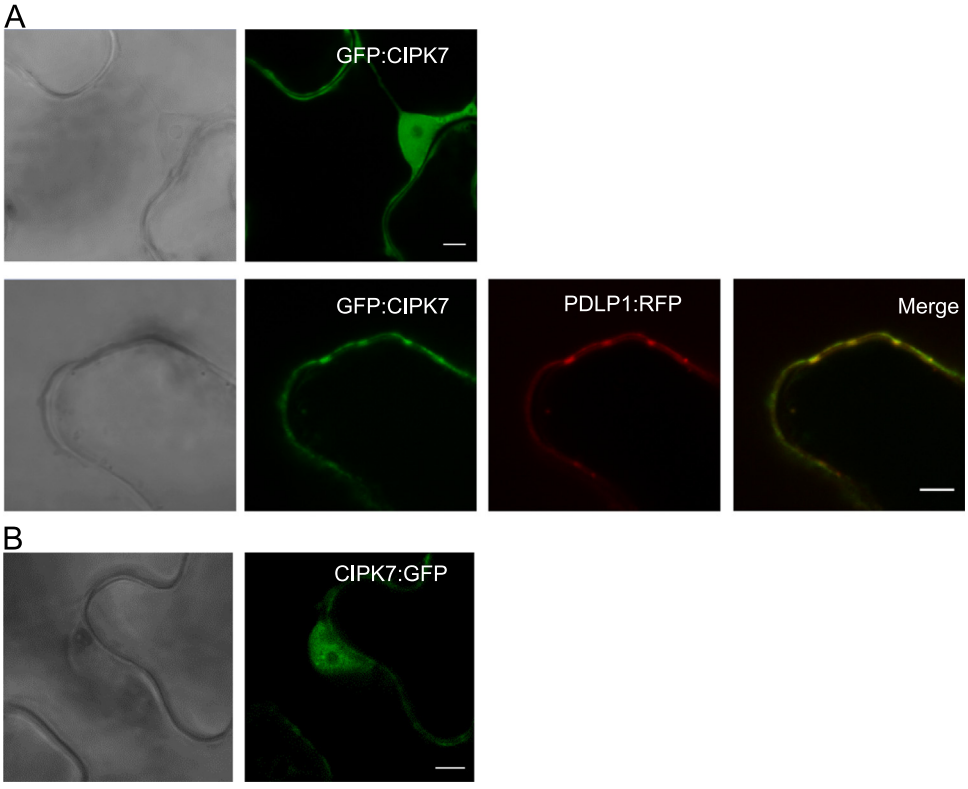

Fig. 5. Subcellular localization of AtCIPK7 in *N. benthamiana*. GFP-fusion proteins were transiently expressed in *N. benthamiana* leaves and epidermal cells were observed under confocal microscopy. (A) Infiltration of GFP:CIPK7 (upper panels). Co-infiltration of GFP:CIPK7 with the plasmodesmata marker PDLP1 (lower panels); (B) Infiltration of CIPK:GFP. Bright-field images are presented on the left. Expression of the fusion proteins was confirmed by Western-blot (Fig. S2). Bars represent 5 μm.

latter domain includes a NAF domain (also known as a FISL motif), responsible for interaction with CBLs, and a protein-phosphatase interaction (PPI) domain mediating CIPK interaction with phosphatases (Albrecht et al., 2001; Ohta et al., 2003). Interaction between the kinase active site and its regulatory domain seems to maintain the kinase protein in an inactive state, whereas binding to CBL breaks the interaction between the two domains and activates the kinase (Gong et al., 2002; Guo et al., 2001). We observed that RT_{Cter} of TuYV does not bind the CBL-binding domain but a peptide encompassing the PPI domain of AtCIPK7. This suggests that the viral protein could regulate the activity of the phosphatase.

Transient overexpression of the AtCIPK7 protein fused to GFP in *N. benthamiana* led to a local increase of TuYV and also of BMYV, a polerovirus closely related to TuYV. While both GFP-CIPK fusion proteins increased BMYV accumulation, TuYV titer elevation was only observed when GFP was fused to the N-terminus of AtCIPK7 and not to its C-terminus. This suggests that, in the specific case of TuYV, AtCIPK7's require a free C-terminus which is in agreement with the experiments performed in yeast, which showed that the C- and not the N-terminal domain of the kinase interacts with RT_{Cter} of TuYV. Additionally the positive effect of AtCIPK7 on the virus titer was not observed on a TuYV mutant lacking RT_{Cter} (TuYV-ΔRT_{Cter}). This confirms that GFP:CIPK7 interacts specifically with the TuYV-RT_{Cter} domain and reinforces the assumption that the local virus titer increase is a consequence of this interaction. The difference observed between TuYV and BMYV could be related to a different conformation of the C-terminal domain of the RT proteins which in the case of BMYV could interact with both fusion proteins whereas TuYV-RT_{Cter} would bind only GFP:CIPK7. The effect on virus accumulation could be due to an increase in virus replication and/or stability in the infected cells although we observed no significant difference in viral accumulation between the mutant lacking this domain and the wild-type virus in protoplasts or in inoculated leaves (see Fig. 1 and Table 1). Since the elevated TuYV titer observed in the presence of GFP:CIPK7 did not promote virus exit from infected cells, another hypothesis is that overexpression of AtCIPK7 could be responsible for a partial hindrance of virus exit resulting in an over-accumulation of the virus in the inoculated cells. Detection of GFP:CIPK7 in or close to plasmodesmata is in agreement with this idea. However for practical reasons we performed the sub-cellular localization in mesophyll cells, and not in phloem cells. As plasmodesmata of mesophyll cells and those connecting sieve tubes and companion cells are physically and physiologically diverse (Beebe and Russin, 1999; Oparka and Cruz, 2000; Roberts and Oparka, 2003), we cannot assert that CIPK7 has the same localization in both cell types. The hypothesis of physical hindrance of viral exit by CIPK7 would support the concept of AtCIPK7 being a plant defense protein limiting TuYV movement in the plant by targeting the RT_{Cter} domain. The TuYV-ΔRT_{Cter} mutant lacking the CIPK7 recognition domain would not be targeted by this defense mechanism and, as experimentally observed, its local accumulation was not affected by the kinase overexpression. When analyzing CIPK7 mRNA expression in TuYV infected plants, we observed a moderate reduction in the accumulation of AtCIPK7 mRNA, 21 days after virus inoculation, which could correspond to a virus counter-mechanism to impede the action of the kinase. Considering the phloem-restriction of this virus, it is still conceivable that the AtCIPK7 mRNA is more tightly regulated in infected phloem cells than in other cell types, an effect that would be minored in the global analysis performed here.

The specific binding between AtCIPK7 and RT_{Cter} observed in yeast and *in planta* may reflect, during the virus cycle, an interaction with either the C-terminal part of the RT protein as a cleaved peptide or with the complete RT protein. Since RT_{Cter} has never been detected in infected plants, either because of a lack of sensitivity of the detection techniques or because of a rapid degradation of this product, interaction of AtCIPK7 with the complete RT protein is more likely.

The full-length RT protein has previously been demonstrated to be multifunctional (Brault et al., 1995; Bruyère et al., 1997; Mutterer et al., 1999; Peter et al., 2009, 2008). The data presented in this manuscript add more complexity to the functions of the full-length RT protein. In addition to its implication in aphid transmission and virus movement, it could either promote virus accumulation in the infected cells or more likely be the target of a plant defense mechanism to limit virus exit from infected cells.

Involvement of a CIPK protein in viral infection is a novel concept that has only been reported for *Cucumber mosaic virus* (CMV). The CMV polymerase 2a protein was identified as an interacting partner of the tobacco NtCIPK12 homolog (Kang et al., 2012). The C-terminus of NtCIPK12 was able to phosphorylate the 2 a protein *in vitro* (Kang et al., 2012) suggesting a potential mechanism of antiviral resistance in the plant since phosphorylation of the 2a protein inhibits formation of the replication complex (Kim et al., 2002). Further examination of the RT protein phosphorylation status by AtCIPK7 should bring more insights into the biological function of AtCIPK7 in the TuYV cycle.

Experimental procedures

Viral mutant construct and plant inoculation

To obtain TuYV-ΔRT_{Cter}, the TuYV mutant bearing a deletion of the C-terminal part of the RT protein (RT_{Cter}), conventional PCR cloning techniques were employed. The plasmid pBWNhe/Mlu (referred thereafter as pTuYV-NM), containing the full-length sequence of TuYV (previously referred to as *Beet western yellows virus*) with two additional restriction sites NheI and MluI (Brault et al., 2005) was used as template for PCR amplification using the oligonucleotides listed in Table S4. The PCR fragment was digested by NheI and MluI enzymes and introduced into the NheI-MluI-digested pTuYV-NM to yield the pTuYV-ΔRT_{Cter}. To generate the plasmid used for agroinoculation, the SpeI–SalI fragment from pTuYV-ΔRT_{Cter} was subsequently subcloned into pBinTuYV-GΔRN (Leiser et al., 1992) digested with the same enzymes. The plasmid constructs were verified by DNA sequencing. The resulting plasmid was introduced into *Agrobacterium tumefaciens* C58C1 (Holsters et al., 1980) for agroinoculation. A binary construct containing the full-length clone of *Beet mild yellowing virus* (BMYV) and introduced into *A. tumefaciens* was also used in the agroinoculation experiments (Klein et al., 2014). *A. tumefaciens* harboring the binary plasmids was grown to an optical density (OD) at 600 nm of 0.5 and agroinfiltrated into different plant species (English et al., 1997). Inoculated plants were assayed by double-antibody sandwich enzyme-linked immunosorbent assay (DAS-ELISA) (Clark and Adams, 1977) with an antiserum raised against TuYV (Loewe, Kronach, Germany). For each plant, 3 to 4 pieces of different leaves were collected and ground together. *A. thaliana* Col-0 was also inoculated with TuYV using 5 aphids per plant which had previously been fed on purified virus (50 μg/ml) (Bruyère et al., 1997).

Protoplast infection and viral protein detection

Protoplasts of *Chenopodium quinoa* were inoculated with viral RNA transcripts by electroporation as described by Bruyère et al. (1997). Proteins were extracted from 50,000 protoplasts 72 h after inoculation and analyzed by Western blot using coat protein- and RT-specific antibodies (Reutenauer et al., 1993).

Yeast two-hybrid assay and protein detection in yeast

Total RNA was extracted from fluorescent protoplasts expressing the GFP under the control of the AtSUC2 companion cell specific promoter (Chapuis et al., in preparation) using a RNeasy Plant mini kit (Qiagen) and following the manufacturer's instructions. Isolated RNA was used to construct an *A. thaliana* companion cell specific cDNA library in the pGADT7 vector, directly in *Saccharomyces cerevisiae* strain Y187, following the protocol from the "Mate and Plate" library system (Clontech). Y2HGold yeast cells, containing the reporter genes *HIS3* and *ADE2*, were transformed with a construct expressing the C-terminal part of the RT protein sequence (nts 4768–5495) fused to the GAL4 DNA binding domain (BD) into the pGBKT7 vector, and the resulting fusion protein was used as a bait. The phloem cDNA library was screened against the bait by yeast mating using the Matchmaker™ Gold Yeast Two-Hybrid Gal4 promoter-based system (Clontech) as described by the manufacturer. Selection of the colonies in which interactions occurred was made by plating yeast cells onto minimal synthetically defined medium for yeast (SD medium) deprived of leucine, tryptophan, histidine and adenine [-LWHA]. The prey fragments of the yeast clones developing on the selective media were amplified by PCR and sequenced. The resulting sequences were used to identify the corresponding interacting proteins in the GenBank database.

The N-terminal domain of AtCIPK7 covering the first 283 amino acid residues was amplified by RT-PCR and cloned into the pGADT7 vector between EcoRI and BamHI sites to yield pGAD-CIPK7$_{1\text{-}283}$ using the primers listed in Table S4. The AtCIPK7 full-length sequence, cloned into the pGAD.GH vector (pGAD-CIPK7-FL$_{1\text{-}429}$), was kindly provided by Kudla.

In order to test the interaction of pGAD-CIPK7-FL$_{1\text{-}429}$, pGAD-CIPK7$_{1\text{-}283}$, and pGAD-CIPK7$_{346\text{-}429}$ with pGBKT7-RT$_{Cter}$, Y2HGold yeast cells were co-transformed with one of the pGAD-derived constructs and with pGBKT7-RT$_{Cter}$ using the lithium acetate method. Co-transformed yeast cells were selected on SD medium lacking leucine and tryptophan [-LW] before being spotted onto SD [-LWHA] after serial dilutions in 2% glucose (A_{600}= 1 to 10^{-4}). Yeast cells were grown at 23 °C for 8 days. All experiments were performed in triplicate. Empty pGADT7 or pGAD. GH vectors were used as negative controls.

GFP- and RFP-fusion constructs and N. benthamiana infiltration

The full-length coding sequence of AtCIPK7 was amplified by RT-PCR from total RNA extracted from *A. thaliana* (RNeasy plant mini kit, Qiagen). AtCIPK7 constructs fused to GFP and RT$_{Cter}$ (nt 4767 to 5495) fused to RFP were generated by the Gateway technology according to the manufacturer's instructions (Invitrogen). Briefly, the AtCIPK7 and the RT$_{Cter}$ sequences were recombined into the Gateway donor plasmid pDONR207 (Invitrogen) to yield entry clones which were subsequently analyzed by sequencing. The entry clones were further used for recombination with the destination vectors pK7WGF2 or pK7FWG2 for expression of AtCIPK7 fused with GFP at, respectively, its N- or C-terminus and pH7WGR2 for expression of RT$_{Cter}$ fused with RFP at its N-terminus (Karimi et al., 2002). The primers containing attB1 and attB2 recombination sequences that were used to generate Gateway constructs are listed in Table S4.

A. tumefaciens C58C1 was transformed with the recombinant Gateway constructs and three to four week old *N. benthamiana* plants infiltrated (English et al., 1997). All infiltrations were performed in the presence of the RNA silencing suppressor of *Tobacco bushy stunt virus*, the P19 protein.

Immunoprecipitation

Immunoprecipitation was done on *N. benthamiana* leaves 3 days after infiltration using anti-GFP microbeads (Miltenyi Biotec) according manufacturer's instructions, except for lysis and washing buffers. Briefly, samples were ground in liquid nitrogen and extracted with lysis buffer [150 mM NaCl, 1% NP40, 10% glycerol, 50 mM Tris HCl (pH 7.5)]. A cocktail of antiproteases EDTA free (Roche) and 10 μM MG132 were also added to prevent protein degradation. The mixtures were incubated at 4 °C with gentle shaking for 1 h. The immunocomplex was captured by adding 50 μl of anti-GFP microbeads (Miltenyi Biotec) and incubated at 4 °C for 30 min. Magnetically-labeled proteins were retained on a micro column placed in the magnetic field of a μMACS Separator. Columns were washed 3 times at 4 °C with lysis buffer. Proteins immunoprecipitated were directly eluted and solubilized with 50 μl of elution buffer prior to 10% SDS-PAGE and transfer onto nitrocellulose. Detection was performed using in-house made GFP antibodies provided by the "Institut de Biologie Moléculaire des Plantes" (IBMP-CNRS, Strasbourg, France) and anti-RFP antibodies (Living Colors® DsRed Polyclonal Antibody, Clontech). The protein/antibody complex was detected by chemiluminescence (Lumi-LightPLUS kit, Roche) after addition of a goat anti-rabbit IgG-HRP conjugate (Invitrogen) using a G:box camera (Syngene).

Subcellular localization by confocal microscopy

N. benthamiana was infiltrated with GFP:CIPK7 or CIPK7:GFP in the presence of the P19 protein. Images were acquired 48 h after infiltration using a laser scanning confocal microscope (Zeiss) with software package LSM510 (version 2.8), equipped with a 63 × water-corrected objective in multitrack mode. eGFP was excited with the 488 nm line of an Argon laser and detected via a 505–530 nm band emission pass filter.

qRT-PCR analysis of CIPK7 expression in TuYV infected plants

Total RNA was isolated from young leaves collected from mock-inoculated and virus-infected *A. thaliana* using an RNeasy Plant mini kit (Qiagen) and following the manufacturer's instructions. On-column DNase treatment using RNase-free DNase set (Qiagen) was performed. Three biological samples were analyzed per treatment and each sample represented a pool of RNA isolated from three plants. The presence of TuYV was tested by RT-PCR before pooling the RNA extracts. Complementary DNA was synthesized from 1 μg total RNA using oligo (dT) primers and SuperScript® III reverse transcriptase (Invitrogen) according to the manufacturer's instructions. qPCR primers were designed using ProbeFinder 2.45 (Roche Applied Sciences) (Table S4). Specificity of PCR primers was assessed by melting curve analysis of PCR products. PCR was performed using the Bio-Rad CFX96 Touch™ Real-Time PCR Detection System and SsoFast™ EvaGreen® Supermix (Bio-Rad). Ten microliters of PCR reaction contained 12.5 ng cDNA, 400 nM primers and 5 μl SsoFast EvaGreen supermix. Average amplification efficiency was determined by LinRegPCR. Relative expression levels were normalized to *At4g26410* (Czechowski et al., 2005), whose cycle threshold (C_T) value was subtracted from the C_T value of *AtCIPK7*, yielding a ΔC_T value. The relative expression levels of *AtCIPK7* were calculated using the $\Delta\Delta C_T$ method. The qPCR cycles were set up as follows: 95 °C for 30 s followed by 40 cycles at the following conditions: 95 °C for 5 s, 61 °C for 5 s and 77 °C for 5 s; melt curve analysis was performed at 55 °C to 95 °C in 0.5 °C increments for 5 s.

T-DNA mutant characterization

The *A. thaliana* T-DNA insertion mutant *cipk7* (SALK_124117) in Col-0 background was obtained from the Arabidopsis Biological Resource Center (ABRC) (Alonso et al., 2003). Insertion of the T-DNA sequence into the CIPK7 sequence of the *cipk7* mutant was controlled by PCR genotyping using gene-specific primers and left border primers of the T-DNA insertion (LBb1) (Table S4). The absence of expression of AtCIPK7-mRNA in *cipk7* mutant was controlled by RT-PCR on total RNA extracts (RNeasy Plant mini kit, Qiagen), and RNA integrity was confirmed by RT-PCR amplification of actin mRNA. All primers are described in Table S4.

Acknowledgments

We thank Jörg Kudla (Münster University, Münster) for sharing the AtCIPK7 full-length clone, critical reading of the manuscript and fruitful discussions. Christophe Ritzenthaler (IBMP, Strasbourg) is acknowledged for providing the marker used in confocal microscopy and Manfred Heinlein (IBMP, Strasbourg) for reading the manuscript. GFP antibodies were kindly provided by Danièle Scheidecker (IBMP, Strasbourg). We are grateful to Norbert Sauer (MPP, Erlangen) for providing AtSUC2:GFP plants and to Marion Clavel (IBMP, Strasbourg) for technical assistance with the immunoprecipitation experiment. We would also like to thank Nicole Bochet and the members of the experimental unit of INRA-Colmar for their implication in virus purification, aphids rearing and plant production. We are also grateful to Danica Goggin (University of Western Australia) for English proofreading of the manuscript. C. R-M, D. G and S. C were financed by The French National Research Agency (ANR) in the frame of the ViroMouv project (ANR-08-GENM-016-003).

Appendix A. Supplementary material

Supplementary data associated with this article can be found in the online version at http://dx.doi.org/10.1016/j.virol.2015.08.031.

References

Albrecht, V., Ritz, O., Linder, S., Harter, K., Kudla, J., 2001. The NAF domain defines a novel protein–protein interaction module conserved in Ca^{2+}-regulated kinases. EMBO J. 20, 1051–1063.

Alonso, J.M., Stepanova, A.N., Leisse, T.J., Kim, C.J., Chen, H., Shinn, P., Stevenson, D. K., Zimmerman, J., Barajas, P., Cheuk, R., Gadrinab, C., Heller, C., Jeske, A., Koesema, E., Meyers, C.C., Parker, H., Prednis, L., Ansari, Y., Choy, N., Deen, H., Geralt, M., Hazari, N., Hom, E., Karnes, M., Mulholland, C., Ndubaku, R., Schmidt, I., Guzman, P., Aguilar-Henonin, L., Schmid, M., Weigel, D., Carter, D.E., Marchand, T., Risseeuw, E., Brogden, D., Zeko, A., Crosby, W.L., Berry, C.C., Ecker, J.R., 2003. Genome-wide insertional mutagenesis of *Arabidopsis thaliana*. Science 301, 653–657.

Amari, K., Boutant, E., Hofmann, C., Schmitt-Keichinger, C., Fernandez-Calvino, L., Didier, P., Lerich, A., Mutterer, J., Thomas, C.L., Heinlein, M., Mely, Y., Maule, A.J., Ritzenthaler, C., 2010. A family of plasmodesmal proteins with receptor-like properties for plant viral movement proteins. PLoS Pathog. 6, e1001119.

Batistic, O., Kudla, J., 2012. Analysis of calcium signaling pathways in plants. Biochim. Biophys. Acta 1820, 1283–1293.

Baumberger, N., Tsai, C.H., Lie, M., Havecker, E., Baulcombe, D.C., 2007. The Polerovirus silencing suppressor P0 targets ARGONAUTE proteins for degradation. Curr. Biol. 17, 1609–1614.

Beebe, D.U., Russin, W.A., 1999. Plasmodesmata in the phloem-loading pathway. In: Van Bel, A.J.E., van Kesteren, W.J.P. (Eds.), Plasmodesmata: Structure, Function, Role in Cell Communication. Springer-Verlag, New-York, pp. 261–293.

Boissinot, S., Erdinger, M., Monsion, B., Ziegler-Graff, V., Brault, V., 2014. Both structural and non-structural forms of the readthrough protein of cucurbit aphid-borne yellows virus are essential for efficient systemic infection of plants. PloS ONE 9, e93448.

Bortolamiol, D., Pazhouhandeh, M., Marrocco, K., Genschik, P., Ziegler-Graff, V., 2007. The Polerovirus F box protein P0 targets ARGONAUTE1 to suppress RNA silencing. Curr. Biol. 17, 1615–1621.

Brault, V., Perigon, S., Reinbold, C., Erdinger, M., Scheidecker, D., Herrbach, E., Richards, K., Ziegler-Graff, V., 2005. The Polerovirus minor capsid protein determines vector specificity and intestinal tropism in the aphid. J. Virol. 79, 9685–9693.

Brault, V., van den Heuvel, J.F., Verbeek, M., Ziegler-Graff, V., Reutenauer, A., Herrbach, E., Garaud, J.C., Guilley, H., Richards, K., Jonard, G., 1995. Aphid transmission of beet western yellows luteovirus requires the minor capsid readthrough protein P74. EMBO J. 14, 650–659.

Bruyère, A., Brault, V., Ziegler-Graff, V., Simonis, M.T., Van den Heuvel, J.F., Richards, K., Guilley, H., Jonard, G., Herrbach, E., 1997. Effects of mutations in the beet western yellows virus readthrough protein on its expression and packaging and on virus accumulation, symptoms, and aphid transmission. Virology 230, 323–334.

Chapuis S., Monsion B., Halter D., Rodriguez-Medina C., Baldenweck R., Thébaud G., Hugueney P., Revers F., Brault V. and Ziegler-Graff V. Profiling of phloem specific gene expression upon polerovirus infection, manuscript in preparation.

Chay, C.A., Gunasinge, U.B., Dinesh-Kumar, S.P., Miller, W.A., Gray, S.M., 1996. Aphid transmission and systemic plant infection determinants of barley yellow dwarf luteovirus-PAV are contained in the coat protein readthrough domain and 17-kDa protein, respectively. Virology 219, 57–65.

Clark, M.F., Adams, A.N., 1977. Characteristics of the microplate method of enzyme-linked immunosorbent assay for the detection of plant viruses. J. Gen. Virol. 34, 475–483.

Csorba, T., Lozsa, R., Hutvagner, G., Burgyan, J., 2010. Polerovirus protein P0 prevents the assembly of small RNA-containing RISC complexes and leads to degradation of ARGONAUTE1. Plant J 62, 463–472.

Czechowski, T., Stitt, M., Altmann, T., Udvardi, M.K., Scheible, W.R., 2005. Genome-wide identification and testing of superior reference genes for transcript normalization in Arabidopsis. Plant Physiol. 139, 5–17.

D'Angelo, C., Weinl, S., Batistic, O., Pandey, G.K., Cheong, Y.H., Schultke, S., Albrecht, V., Ehlert, B., Schulz, B., Harter, K., Luan, S., Bock, R., Kudla, J., 2006. Alternative complex formation of the Ca-regulated protein kinase CIPK1 controls abscisic acid-dependent and independent stress responses in Arabidopsis. Plant J. 48, 857–872.

English, J.J., Davenport, G.F., Elmayan, T., Vaucheret, H., Baulcombe, D.C., 1997. Requirement of sense transcription for homology-dependent virus resistance and trans-inactivation. Plant J. 12, 597–603.

Gildow, F., 1999. Luteovirus transmission mechanisms regulating vector specificity. In: Smith, H.G., Barker, H. (Eds.), The Luteoviridae. CAB International, Oxon, UK, pp. 88–111.

Gong, D., Guo, Y., Jagendorf, A.T., Zhu, J.K., 2002. Biochemical characterization of the Arabidopsis protein kinase SOS2 that functions in salt tolerance. Plant Physiol. 130, 256–264.

Guo, Y., Halfter, U., Ishitani, M., Zhu, J.K., 2001. Molecular characterization of functional domains in the protein kinase SOS2 that is required for plant salt tolerance. Plant Cell 13, 1383–1400.

Halfter, U., Ishitani, M., Zhu, J.K., 2000. The Arabidopsis SOS2 protein kinase physically interacts with and is activated by the calcium-binding protein SOS3. Proc. Natl. Acad. Sci. U.S.A. 97, 3735–3740.

Holsters, M., Silva, B., Van Vliet, F., Genetello, C., De Block, M., Dhaese, P., Depicker, A., Inze, D., Engler, G., Villarroel, R., et al., 1980. The functional organization of the nopaline *A. tumefaciens* plasmid pTiC58. Plasmid 3, 212–230.

Hruz, T., Laule, O., Szabo, G., Wessendorp, F., Bleuler, S., Oertle, L., Widmayer, P., Gruissem, W., Zimmermann, P., 2008. Genevestigator v3: a reference expression database for the meta-analysis of transcriptomes. Adv. Bioinform. 2008, 420747.

Imlau, A., Truernit, E., Sauer, N., 1999. Cell-to-cell and long-distance trafficking of the green fluorescent protein in the phloem and symplastic unloading of the protein into sink tissues. Plant Cell 11, 309–322.

Kang, H.K., Yang, S.H., Lee, Y.P., Park, Y.I., Kim, S.H., 2012. A tobacco CBL-interacting protein kinase homolog is involved in phosphorylation of the N-terminal domain of the cucumber mosaic virus polymerase 2a protein. Biosci. Biotechnol. Biochem. 76, 2101–2106.

Karimi, M., Inze, D., Depicker, A., 2002. GATEWAY vectors for Agrobacterium-mediated plant transformation. Trends Plant Sci. 7, 193–195.

Kim, S.H., Palukaitis, P., Park, Y.I., 2002. Phosphorylation of cucumber mosaic virus RNA polymerase 2a protein inhibits formation of replicase complex. EMBO J. 21, 2292–2300.

Klein, E., Brault, V., Klein, D., Weyens, G., Lefebvre, M., Ziegler-Graff, V., Gilmer, D., 2014. Divergence of host range and biological properties between natural isolate and full-length infectious cDNA clone of the Beet mild yellowing virus 2ITB. Mol. Plant Pathol. 15, 22–30.

Kolukisaoglu, U., Weinl, S., Blazevic, D., Batistic, O., Kudla, J., 2004. Calcium sensors and their interacting protein kinases: genomics of the Arabidopsis and rice CBL-CIPK signaling networks. Plant Physiol. 134, 43–58.

Kudla, J., Xu, Q., Harter, K., Gruissem, W., Luan, S., 1999. Genes for calcineurin B-like proteins in Arabidopsis are differentially regulated by stress signals. Proc. Natl. Acad. Sci. U.S.A. 96, 4718–4723.

Lee, L., Palukaitis, P., Gray, S.M., 2002. Host-dependent requirement for the Potato leafroll virus 17-kda protein in virus movement. Mol. Plant Microbe Interact. 15, 1086–1094.

Leiser, R.M., Ziegler-Graff, V., Reutenauer, A., Herrbach, E., Lemaire, O., Guilley, H., Richards, K., Jonard, G., 1992. Agroinfection as an alternative to insects for

infecting plants with beet western yellows luteovirus. Proc. Natl. Acad. Sci. U.S. A. 89, 9136–9140.
Liu, J., Ishitani, M., Halfter, U., Kim, C.S., Zhu, J.K., 2000. The Arabidopsis thaliana SOS2 gene encodes a protein kinase that is required for salt tolerance. Proc. Natl. Acad. Sci. U.S.A. 97, 3730–3734.
Mutterer, J.D., Stussi-Garaud, C., Michler, P., Richards, K.E., Jonard, G., Ziegler-Graff, V., 1999. Role of the beet western yellows virus readthrough protein in virus movement in Nicotiana clevelandii. J. Gen. Virol. 80, 2771–2778.
Ohta, M., Guo, Y., Halfter, U., Zhu, J.K., 2003. A novel domain in the protein kinase SOS2 mediates interaction with the protein phosphatase 2C ABI2. Proc. Natl. Acad. Sci. U.S.A. 100, 11771–11776.
Oparka, K.J., Cruz, S.S., 2000. THE GREAT ESCAPE: phloem transport and unloading of macromolecules1. Annu. Rev. Plant Physiol. Plant Mol. Biol. 51, 323–347.
Pazhouhandeh, M., Dieterle, M., Marrocco, K., Lechner, E., Berry, B., Brault, V., Hemmer, O., Kretsch, T., Richards, K.E., Genschik, P., Ziegler-Graff, V., 2006. F-box-like domain in the polerovirus protein P0 is required for silencing suppressor function. Proc. Natl. Acad. Sci. U.S.A. 103, 1994–1999.
Peter, K.A., Gildow, F., Palukaitis, P., Gray, S.M., 2009. The C terminus of the polerovirus p5 readthrough domain limits virus infection to the phloem. J. Virol. 83, 5419–5429.
Peter, K.A., Liang, D., Palukaitis, P., Gray, S.M., 2008. Small deletions in the potato leafroll virus readthrough protein affect particle morphology, aphid transmission, virus movement and accumulation. J. Gen. Virol. 89, 2037–2045.
Quan, R., Lin, H., Mendoza, I., Zhang, Y., Cao, W., Yang, Y., Shang, M., Chen, S., Pardo, J.M., Guo, Y., 2007. SCABP8/CBL10, a putative calcium sensor, interacts with the protein kinase SOS2 to protect Arabidopsis shoots from salt stress. Plant Cell 19, 1415–1431.
Reinbold, C., Lacombe, S., Ziegler-Graff, V., Scheidecker, D., Wiss, L., Beuve, M., Caranta, C., Brault, V., 2013. Closely related poleroviruses depend on distinct translation initiation factors to infect Arabidopsis thaliana. Mol. Plant Microbe Interact. 26, 257–265.
Reutenauer, A., Ziegler-Graff, V., Lot, H., Scheidecker, D., Guilley, H., Richards, K., Jonard, G., 1993. Identification of beet western yellows luteovirus genes implicated in viral replication and particle morphogenesis. Virology 195, 692–699.
Revollon, S., Strub, J.M., Fitchette, A.C., Wiss, L., Gomord, V., Van Dorsselaer, A., Brault, V., 2010. A reinvestigation provides no evidence for sugar residues on structural proteins of poleroviruses and argues against a role for glycosylation of virus structural proteins in aphid transmission. Virology 402, 303–314.
Roberts, A.G., Oparka, K., 2003. Plasmodesmata and the control of symplastic transport. Plant Cell Environ. 26, 103–124.
Schmitz, J., Stussi-Garaud, C., Tacke, E., Prufer, D., Rohde, W., Rohfritsch, O., 1997. In situ localization of the putative movement protein (pr17) from potato leafroll luteovirus (PLRV) in infected and transgenic potato plants. Virology 235, 311–322.
The Arabidopsis thaliana salt tolerance gene SOS1 encodes a putative Na^+/H^+ antiporter. Proc. Natl. Acad. Sci. U.S.A. 97, 6896–6901.
Sokolova, M., Prufer, D., Tacke, E., Rohde, W., 1997. The potato leafroll virus 17K movement protein is phosphorylated by a membrane-associated protein kinase from potato with biochemical features of protein kinase C. FEBS Lett. 400, 201–205.
Tacke, E., Prufer, D., Schmitz, J., Rohde, W., 1991. The potato leafroll luteovirus 17K protein is a single-stranded nucleic acid-binding protein. J. Gen. Virol. 72, 2035–2038.
Tacke, E., Schmitz, J., Prufer, D., Rohde, W., 1993. Mutational analysis of the nucleic acid-binding 17 kDa phosphoprotein of potato leafroll luteovirus identifies an amphipathic alpha-helix as the domain for protein/protein interactions. Virology 197, 274–282.
Wang, J.Y., Chay, C., Gildow, F.E., Gray, S.M., 1995. Readthrough protein associated with virions of barley yellow dwarf luteovirus and its potential role in regulating the efficiency of aphid transmission. Virology 206, 954–962.
Weinl, S., Kudla, J., 2009. The CBL-CIPK $Ca(2+)$-decoding signaling network: function and perspectives. New Phytol. 184, 517–528.
Ziegler-Graff, V., Brault, V., Mutterer, J., Simonis, M.T., Herrbach, E., Guilley, H., Richards, K., Jonard, G., 1996. The coat protein of beet western yellows luteovirus is essential for systemic infection but the viral gene products P29 and P19 are dispensable for systemic infection and aphid transmission. Mol. Plant Microbe Interact. 9, 501–510.